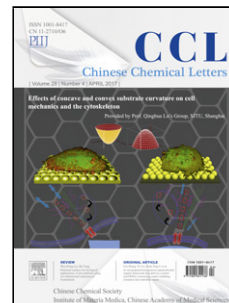


## Accepted Manuscript

Title: Aggregation-induced phosphorescence and mechanochromic luminescence of a tetraphenylethene-based gold(I) isocyanide complex

Author: Wen-Bo Li Wei-Jian Luo Kai-Xuan Li Wang-Zhang  
Yuan Yong-Ming Zhang



PII: S1001-8417(17)30137-7  
DOI: <http://dx.doi.org/doi:10.1016/j.cclet.2017.04.008>  
Reference: CCLET 4044

To appear in: *Chinese Chemical Letters*

Received date: 4-1-2017  
Revised date: 21-2-2017  
Accepted date: 10-4-2017

Please cite this article as: W.-B. Li, W.-J. Luo, K.-X. Li, W.-Z. Yuan, Y.-M. Zhang, Aggregation-induced phosphorescence and mechanochromic luminescence of a tetraphenylethene-based gold(I) isocyanide complex, *Chinese Chemical Letters* (2017), <http://dx.doi.org/10.1016/j.cclet.2017.04.008>

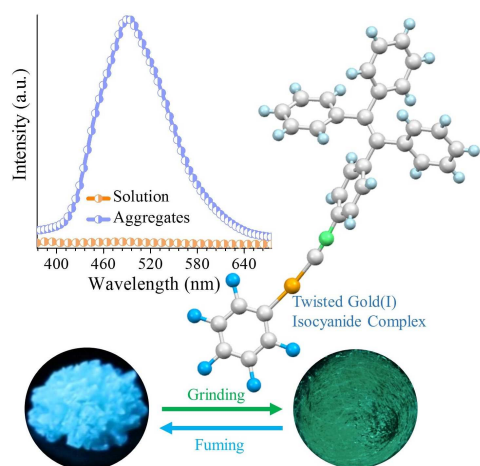
This is a PDF file of an unedited manuscript that has been accepted for publication. As a service to our customers we are providing this early version of the manuscript. The manuscript will undergo copyediting, typesetting, and review of the resulting proof before it is published in its final form. Please note that during the production process errors may be discovered which could affect the content, and all legal disclaimers that apply to the journal pertain.

## Graphical Abstract

Aggregation-induced phosphorescence and mechanochromic luminescence of a tetraphenylethene-based gold(I) isocyanide complex

Wen-Bo Li, Wei-Jian Luo, Kai-Xuan Li, Wang-Zhang Yuan\*, Yong-Ming Zhang\*

Shanghai Key Lab of Electrical Insulation and Thermal Aging, Shanghai Electrochemical Energy Devices Research Center, School of Chemistry and Chemical Engineering, Shanghai Jiao Tong University, Shanghai 200240, China



A new twisted gold(I) isocyanide complex based on tetraphenylethene exhibits aggregation-induced phosphorescence characteristics and reversible mechanochromism between crystalline and amorphous states. Such high contrast mechanism from crystals to amorphous solids upon grinding is resulted from conformation planarization, the enhancement of  $\pi\cdots\pi$  stacking, and the emergence of aurophilic interactions.

Original article

# Aggregation-induced phosphorescence and mechanochromic luminescence of a tetraphenylethene-based gold(I) isocyanide complex

Wen-Bo Li, Wei-Jian Luo, Kai-Xuan Li, Wang-Zhang Yuan\*, Yong-Ming Zhang\*

Shanghai Key Lab of Electrical Insulation and Thermal Aging, Shanghai Electrochemical Energy Devices Research Center, School of Chemistry and Chemical Engineering, Shanghai Jiao Tong University, Shanghai 200240, China

## ARTICLE INFO

## ABSTRACT

## Article history:

Received 4 January 2017

Received in revised form 21 February 2017

Accepted 24 March 2017

Available online

## keywords:

Aggregation-induced phosphorescence

Mechanochromism

Auophilic interaction

Gold(I) isocyanide complex

In this study, a new twisting gold(I) isocyanide complex based on tetraphenylethene (TPE), TPE-NC-Au, was designed and synthesized. It exhibits aggregation induced phosphorescence (AIP) characteristics, owing to the incorporation of Au moiety and conformation rigidification in the aggregated states. Moreover, the emission color of the crystalline solid of TPE-NC-Au changes from blue (454 nm) to green (500 nm) in response to mechanical grinding, due to the combined effects of conformation planarization, enhanced  $\pi\cdots\pi$  stacking, as well as the emergence of auophilic interactions in the ground amorphous state. Notably, the emission color can be restored upon solvent fuming, associating with the reconstruction of crystalline lattices. The AIP and switchable mechanochromism of TPE-NC-Au make it suitable for potential applications in bioimaging, sensing, and optoelectronic devices.

## 1. Introduction

Luminogens with efficient solid-state emission and mechanochromism have attracted great attention owing to their fundamental implications on the molecular packing and potential applications in optical recording, mechanical sensors, security papers, and display devices [1-8]. Researchers have revealed that phase transition between crystalline and amorphous states associating with conformation planarization, supramolecular structure, J-aggregation, and intermolecular  $\pi\cdots\pi$  stacking, *etc.* could be responsible for the mechanochromism [9-13]. Among varying types of luminogens, those with aggregation-induced emission (AIE) features are promising mechanochromic candidates due to their high solid-state efficiencies and normally twisting structures [14-24]. So far, AIE-active mechanochromic luminogens, however, are mostly pure organic compounds, organometallic complexes are still relatively rare, despite they may possess fascinating photophysical properties like phosphorescence [25]. Meanwhile, possible metallophilic interactions in such organometallic complexes may endow the compounds with even obvious mechanochromism [26]. Furthermore, compared with traditional organometallic compounds, for example, the well-known tris(2-phenylpyridine) iridium [Ir(ppy)<sub>3</sub>], whose phosphorescence efficiency is 40% in solution and ~3% when aggregated in films [27,28], AIE metallogens are more emissive in the solid states and thus better high contrast mechanochromic candidates.

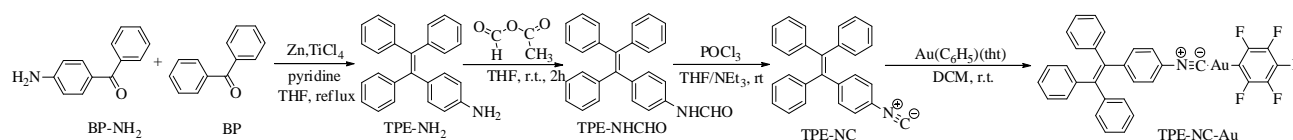
Recently, organometallic complexes with auophilic interactions (Au $\cdots$ Au) between gold centers have attracted considerable interests because of their phosphorescence emission, remarkable mechanochromism, and potential applications to the field of photonic devices [29-33]. To further our understanding on the AIE-active mechanochromic luminogens and gain more insights into the metallophilic interactions, herein, we designed and synthesized a tetraphenylethene (TPE) based gold(I) isocyanide complex (TPE-NC-Au). TPE was chosen because of its typical AIE property, facile synthesis, and versatile functionalization [34-36]. Photophysical properties of the resulting TPE-NC-Au, particularly mechanochromic behaviors were thoroughly investigated.

## 2. Results and discussion

TPE-NC-Au was prepared according to the synthetic route shown in Scheme 1. Briefly, the intermediate product TPE-NH<sub>2</sub> was synthesized by the cross McMurry coupling following the literature procedures [37]. Then, it was amidated and dehydrated successively to yield the key intermediate isocyanide (TPE-NC) [38] with addition of POCl<sub>3</sub> (POCl<sub>3</sub>=phosphorus oxychloride). Further reaction with C<sub>6</sub>F<sub>5</sub>Au(tht) (tht = tetrahydrothiophene) through metal coordination generated the target gold(I) complex of TPE-NC-Au, which was fully characterized by spectroscopic methods and single crystal analysis, with satisfactory results obtained.

\* Corresponding authors.

E-mail address: wzhyuan@sjtu.edu.cn (W.-Z. Yuan), ymzs@sjtu@gmail.com (Y.-M. Zhang).



**Scheme 1.** Synthetic route to TPE-NC-Au.

Due to the incorporation of typical AIE unit of TPE, it is envisaged that TPE-NC-Au is also AIE-active. To check it, its PL emissions in THF and THF/water mixtures with different water fractions ( $f_w$ s) were studied. As shown in Fig. 1, the PL intensity of TPE-NC-Au in THF is weak and not enhanced to a noticeable degree until the  $f_w$  reaches 70%, at which point the molecules begin to aggregate (457 nm, Fig. S10 in Supporting information). At a much higher  $f_w$  of 80%, the PL intensity is greatly enhanced with noticeable green emission peaking at 492 nm. Further addition of even small fraction of water swiftly increases the emission intensity, which is strikingly strengthened by  $\sim 130$ -fold at  $f_w = 90\%$  when compared to that in pure THF. Such an AIE process is also can be identified by the vivid emission contrast depicted in Fig. 1c. While the nonluminescent of TPE-NC-Au in THF solutions can be ascribed to the highly active intramolecular rotations, which can effectively consume exciton energies, the enhanced emission at high  $f_w$ s is associated to the restriction of intramolecular rotations upon aggregation. Further time-resolved emission measurement reveals the phosphorescence nature of the nanosuspensions (107 nm, Fig. S10) in 10/90 THF/water mixture, whose lifetime ( $\tau$ ) is 1.08  $\mu$ s (Fig. S11 in Supporting information). This result also suggests TPE-NC-Au is actually aggregation-induced phosphorescence (AIP) active. Such phosphorescence should be associated with the presence of Au(I), which can promote spin-orbit coupling and subsequent intersystem crossing (ISC) process.

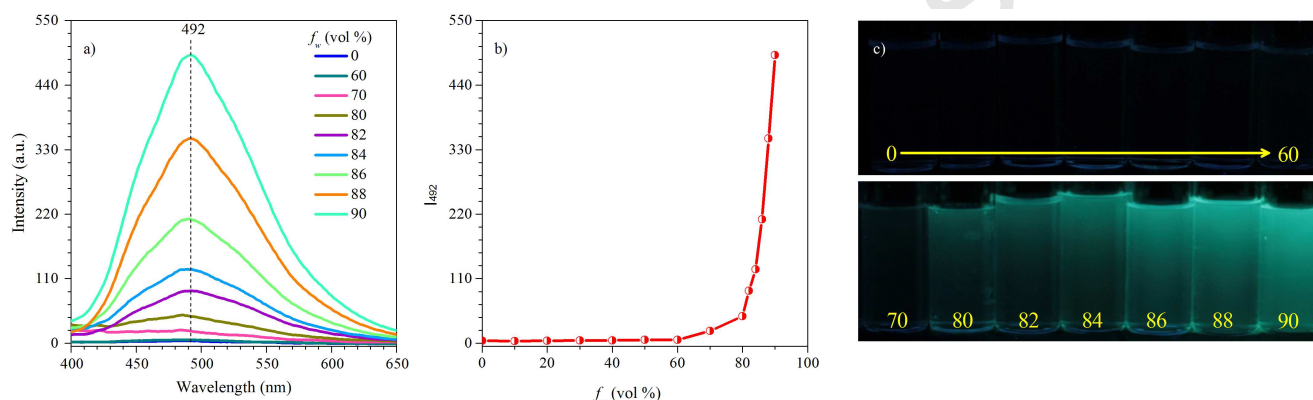


**Fig. 1.** a) PL spectra, b) peak intensities at 492 nm, and c) photographs taken under 365 nm UV lamp of TPE-NC-Au ( $2 \times 10^{-5}$  mol/L) in THF and THF/water mixtures with different  $f_w$ s. For a), excitation wavelength ( $\lambda_{ex}$ ) = 350 nm.

To further quantitatively evaluate the emission of TPE-NC-Au, PL efficiency ( $\Phi$ ) and lifetime of the recrystallized solid were determined, whose values are 21.4% and 1.53  $\mu$ s, respectively, indicative of the relatively high solid-state efficiency and verified phosphorescence feature of TPE-NC-Au. The twisting and Au(I)-containing structure, as well as efficient solid emission renders TPE-NC-Au as promising mechanochromic candidate. Indeed, while the recrystallized solid exhibits strong blue emission with maximum ( $\lambda_{em}$ ) at 454 nm, its ground counterpart demonstrates green emission with red-shifted  $\lambda_{em}$  of 500 nm (Fig. 2a and 2b), which is approaching to those of aggregates in THF/water mixtures (492 nm). Meanwhile, the phosphorescence efficiency is also decreased to 16.5% after grinding. The remarkable differences in emission color, wavelength, and efficiency between the recrystallized and ground samples of TPE-NC-Au illustrate its distinct mechanochromism. Moreover, the emission color of the ground solid can be restored after being fumed with DCM solvent, with slightly blue-shifted  $\lambda_{em}$  (444 nm) when compared to that of the original crystals, indicating the reversible mechanochromism. Further grinding and subsequent fuming cycles illustrate similar emission behaviors, as can be seen from Fig. 2b and 2c, which further confirms the reversible attribute.

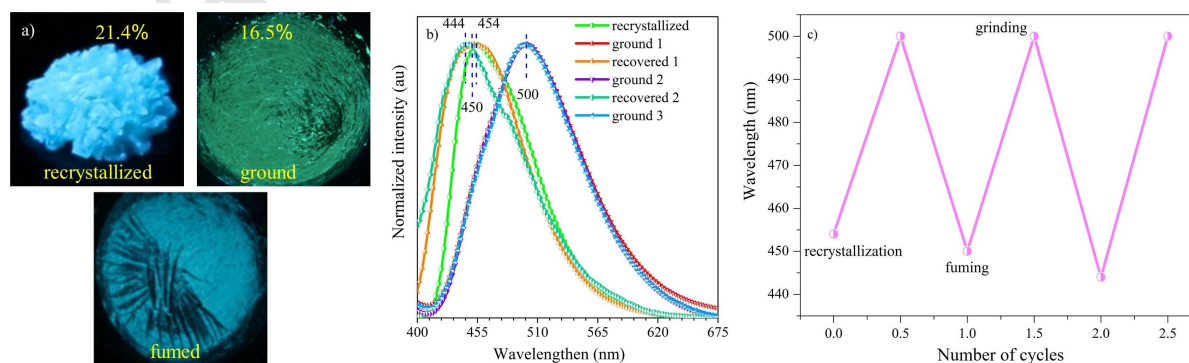


**Fig. 2.** a) Photographs taken under 365 nm UV lamp and b) corresponding PL spectra ( $\lambda_{ex} = 365$  nm) of recrystallized, ground, and fumed solids of TPE-NC-Au. c) Emission maxima of TPE-NC-Au solids at different grinding-fuming cycles.

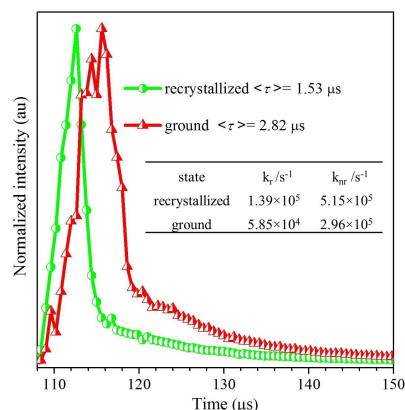


**Fig. 3.** Emission decay curves for recrystallized and ground solids of TPE-NC-Au monitored at 454 and 500 nm, respectively. The inset gives the dynamic photophysical parameters of the solids.  $k_r = \Phi/\tau$ ,  $k_{nr} = 1/\tau - k_r$ .

It is also noted that the lifetime of ground sample (2.82  $\mu$ s) is prolonged with comparison to that of the recrystallized solid. Decreased efficiency along with increased lifetime of the ground sample is highly suggestive of the enhanced exciton coupling upon mechanical stimuli, which may be derived from excimer formation and/or aurophilic interaction. Furthermore, based on the  $\Phi$  and  $\langle\tau\rangle$  values, the radiative/nonradiative rate constants ( $k_r/k_{nr}$ ) are calculated to be  $1.39 \times 10^5/5.15 \times 10^5$  and  $5.85 \times 10^4/2.96 \times 10^5$  s<sup>-1</sup> for the recrystallized and ground solids, respectively (Fig. 3, inset). Clearly, after grinding, the  $k_{nr}$  is even decreased. Therefore, the decline in the efficiency should be mainly ascribed to the decreased  $k_r$ , which is strongly dependent on the oscillator strength. Much stronger exciton coupling would result in lower oscillator strength and thus much smaller  $k_r$ . Based on these results, it is rational to speculate that the conformation planarization and subsequent variations in intermolecular interactions including exciton coupling related  $\pi \cdots \pi$  stacking and aurophilic contacts are responsible for this prominent emission color change from blue to green.

To gain more insights into the mechanochromism of TPE-NC-Au, powder XRD was carried out to study the structural evolution. As shown in Fig. 4, the XRD pattern of the recrystallized sample shows intense and sharp peaks, indicating its ordered molecular packing in the crystalline lattice. Upon grinding, the XRD pattern displays significantly decreased diffraction intensity with a weak halo diffusion at  $2\theta$  of  $\sim 21.4^\circ$ , which implies its disordered amorphous nature. The XRD pattern of the fumed sample, however, is restored with strong and sharp diffractions, which is similar to those of original recrystallized powders. Taken considerations of these results, we can deduce that reversible luminescent color change should be attributed to the switch between ordered crystalline and disordered amorphous states upon mechanical grinding and solvent fuming.

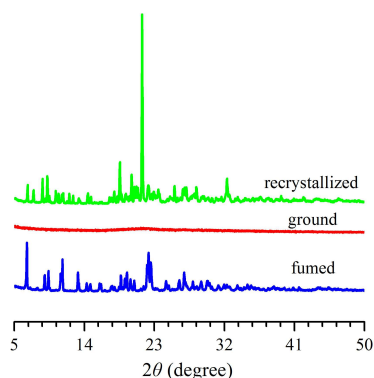


**Fig. 4.** XRD patterns of recrystallized, ground, and fumed solids of TPE-NC-Au.

To further decipher the mechanisms of AIP and particularly mechanochromism of TPE-NC-Au, we cultured the single crystal of it from its DCM solution *via* the solvent diffusion method in the *n*-hexane atmosphere. As can be seen from Fig. 5a, TPE-NC-Au molecules adopt highly twisted conformations with abundant intermolecular interactions such as C-F $\cdots$  $\pi$  (Ar), C-F $\cdots$ N, C-F $\cdots$ C $\equiv$ N, C-H $\cdots$  $\pi$ , C-H $\cdots$ H-C short contacts, and even edge to edge  $\pi \cdots \pi$  interactions. Therefore, the AIE phenomenon can be well rationalized as below: in solutions, the TPE-NC-Au molecules undergo highly active intramolecular rotations, which can effectively consume the exciton energy, thus making them nonemissive; in the aggregated suspensions or solids, these intramolecular rotations can be effectively impeded, particularly in the crystalline state (with assistance of short contacts), thus favoring radiative deactivation of the excitons. Notably, despite  $\pi \cdots \pi$  stacking induced excimer formation is generally harmful to the emission, the whole effect of conformation rigidification overpasses such detrimental effect, thereby offering boosted emission in the aggregated states.

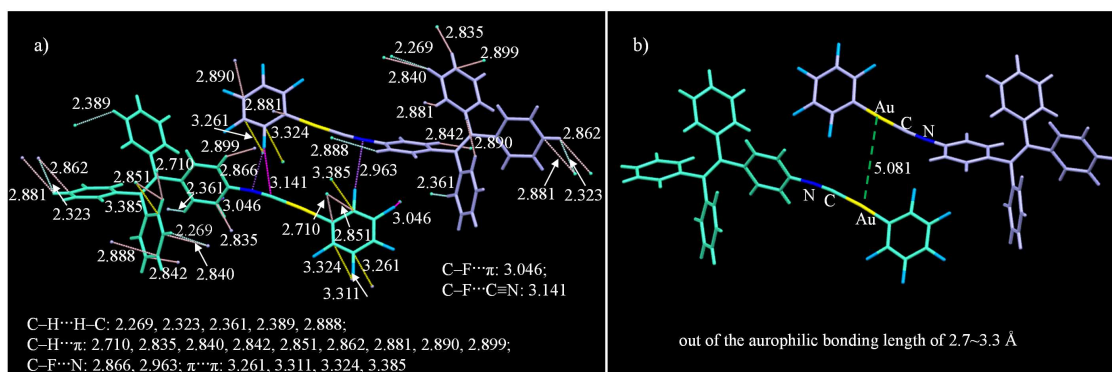


Fig. 5. Single crystal structure (CCDC 1525462) and fragmental molecular packing arrangement of TPE-NC-Au.

On the other hand, for gold(I) isocyanide complexes, auriphilic interactions impact much on the emission, especially on the emission color [39,40]. For TPE-NC-Au crystals, the shortest Au...Au distance of 5.081 Å (Fig. 5b) is far beyond the limited range of auriphilic bonding (2.7–3.3 Å) [32], which indicates the absence of Au...Au interactions. Upon grinding, however, the formation of auriphilic interactions in the amorphous phase becomes possible [31,40], which is further supported by the IR and XPS measurements. The recrystallized sample exhibits an absorption at 2208  $\text{cm}^{-1}$  corresponding to the isocyanide  $\text{N}\equiv\text{C}$  stretching, however, it shifts to higher frequency (2212  $\text{cm}^{-1}$ ) after grinding, suggestive of the formation of auriphilic bonds (Fig. 6a) [31]. Furthermore, the change in the binding energy of the ground sample also supports the assumption of the formation of auriphilic bonds. For the recrystallized sample, the high-resolution XPS spectrum displays binding energies of Au 4f<sub>7/2</sub> and 4f<sub>5/2</sub> at 85.72 and 89.38 eV [41], respectively (Fig. 6b). After grinding, they shift to much lower energies by 0.3 eV and 0.28 eV (Fig. 6b), respectively, which implies enhanced screening effect and thus increased electronic cloud density of Au(I), attributable to the formation of auriphilic bonds. Previous investigations suggest that Au...Au interactions will greatly exert on the emission color [29–33,39,40], which should be aroused from exciton coupling. The red-shifted emission of the ground solid is thus understandable taken considerations into the conformation planarization,  $\pi$ ... $\pi$  stacking, and auriphilic interactions, all of which cooperatively contribute to the emission color change.

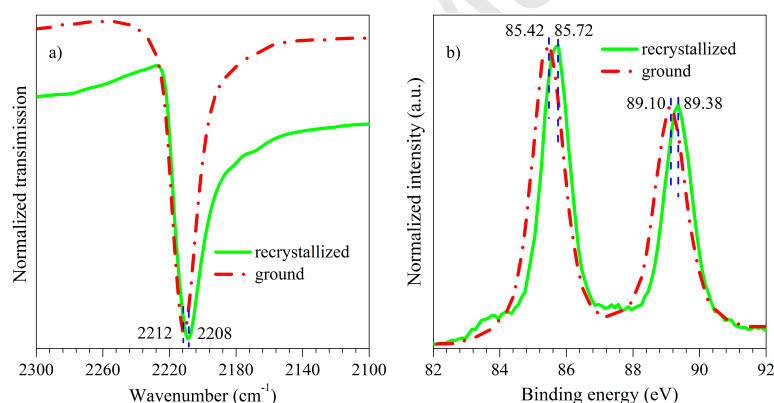


Fig. 6. a) IR and b) Au(I) 4f XPS spectra of recrystallized and ground solids of TPE-NC-Au.

### 3. Conclusion

In summary, highly twisted gold(I) isocyanide complex of TPE-NC-Au has been designed and synthesized. It demonstrates remarkable AIP characteristics with high efficiency of 21.4% in the crystalline state. Moreover, it exhibits reversible and distinct mechanochromism with large emission color/wavelength changes (from blue to green and up to 56 nm). XRD measurement reveals that the phase transition between crystalline and metastable amorphous state before and after grinding is responsible for the mechanochromism. Single crystal data confirm the twisted structure and illustrate abundant intermolecular interactions in the crystals. Upon grinding, while molecular conformations get planarized, most intermolecular interactions are destructed except enhanced  $\pi$ ... $\pi$  stacking, accompanying with emerged auriphilic interactions. Notably, for the first time, XPS spectra are adopted to detect auriphilic interactions in the ground amorphous state. The mechanochromic behavior thus can be well understood in view of conformation planarization, enhanced  $\pi$ ... $\pi$  stacking, and the emergence of auriphilic interactions. Furthermore, this study also indicates an alternative approach, the combination of AIE unit and metallo-moiety, to the fabrication of twisting molecules with AIP properties and high contrast mechanochromism.

### 4. Experimental

#### 4.1 Materials and instruments

Benzophenone (BP) and zinc powder were obtained from Sinopharm Chemical Reagent Co., Ltd. 4-Aminobenzophenone (BP-NH<sub>2</sub>) and phosphorus oxychloride (POCl<sub>3</sub>) were obtained from Acros and Aldrich, respectively. Pyridine, titanium tetrachloride (TiCl<sub>4</sub>), and



petroleum ether (PE) were obtained from Adamas Reagent Ltd. Acetic formic anhydride was prepared from acetic anhydride (0.27 mL, 2.89 mmol, Greagent Co. Ltd) and formic acid (0.11 mL, 2.90 mmol, Greagent Co., Ltd) at 55 °C for 2 h.  $C_6F_5Au(tht)$  was prepared according to the literature [42]. Tetrahydrofuran (THF) was distilled from sodium/BP under nitrogen before use. Triethylamine ( $NEt_3$ ) and dichloromethane (DCM) were distilled under normal pressure from calcium hydride ( $CaH_2$ , Shanghai Lingfeng Chemical Reagent Co. Ltd.). Other commercially available compounds were used as received without further purification.

$^1H$ ,  $^{13}C$ , and  $^{19}F$  NMR spectra were measured on a Bruker ARX 400 NMR spectrometer in chloroform-*d* ( $CDCl_3$ ) using tetramethylsilane (TMS;  $\delta = 0$  ppm) as internal reference. Emission spectra were recorded on a Perkin Elmer LS 55 spectrofluorometer. High resolution mass spectrum (HRMS) was collected on a Fourier Transform ion cyclotron resonance mass spectrometer (Bruker Solarix 7.0T) with MALDI ion source. Powder X-ray diffraction (XRD) data were obtained on a Bruker D8 Advance. Time resolved emission spectra were measured on a PTI QM/TM/IM fluorescence spectrofluorometer. The photoluminescence (PL) quantum yields were determined using an Absolute PLQY C11347 instrument (Hamamatsu, Japan). Single-crystal XRD intensity data were collected on a Bruker SMART APEX diffractometer. XPS were acquired with a Kratos Axis Ultra DLD spectrometer (Kratos Analytical-A Shimadzu group company) using a monochromatic Al  $K\alpha$  source (1486.6 eV).

## 4.2 Synthesis

**TPE-NH<sub>2</sub>:** TPE-NH<sub>2</sub> was synthesized by the typical McMurry reaction according to the literature procedures [34]. Into a two-necked round-bottom flask (100 mL) were added of zinc powder (Zn, 1.49 g, 22.8 mmol) and THF (60 mL). The flask was evacuated and flushed with dry nitrogen three times. After cooling to -5 °C,  $TiCl_4$  was slowly added. The mixture was stirred for 2.5 h at room temperature. After cooling to -5 °C again, pyridine (1.53 mL, 19.0 mmol) was added and the mixture was stirred for 10 min. Then the solution of BP (1.5 g, 7.6 mmol) and BP-NH<sub>2</sub> (1.66 g, 9.1 mmol) in THF (40 mL) was added, the mixture was refluxed overnight. Afterwards,  $K_2CO_3$  solution was added to quench the reaction. After cooling to room temperature, THF was removed by a rotatory evaporator. The solution was poured into water and extracted with DCM. The collected organic layer was dried over anhydrous  $Na_2SO_4$ . After filtration and solvent evaporation, the crude product was purified by silica-gel column chromatography using DCM/PE (1/2, v/v) as eluent. A pale yellow solid was obtained in 72% yield.  $^1H$  NMR (400 MHz,  $CDCl_3$ ):  $\delta$  7.13-6.99 (m, 17H); 6.85-6.82 (d, 2H); 6.52-6.49 (d, 2H).  $^{13}C$  NMR (101 MHz,  $CDCl_3$ ):  $\delta$  144.69, 144.57, 144.52, 144.24, 141.25, 139.87, 135.04, 132.94, 131.89, 131.82, 131.78, 128.20, 128.12, 127.98, 127.96, 126.70, 126.54, 126.53, 115.19. IR (KBr,  $\nu$ ,  $cm^{-1}$ ): 3476, 3378, 3009.

**TPE-NHCHO:** Into a 100 mL two-necked flask were added of TPE-NH<sub>2</sub> (500.0 mg) and THF (30 mL). After cooling to 0 °C, acetic formic anhydride was tardily added by a syringe. The mixture was stirred at room temperature for 2 h. Then the reaction was quenched by the saturated solution of  $NaHCO_3$ . The mixture was extracted with ethyl acetate (EA), then the collected organic layer was dried over anhydrous  $Na_2SO_4$  and concentrated in vacuo. A yellow oil was obtained and used directly for the next step.

**TPE-NC:** Into a 100 mL two-necked flask were added of all crude TPE-NHCHO obtained above, THF (30 mL), and trimethylamine (1.20 mL, 8.6 mmol). The flask was evacuated and flushed with dry nitrogen three times. After cooling to 0 °C,  $POCl_3$  (0.21 mL, 2.2 mmol) was added dropwise. The mixture was stirred for 2 h, then the saturated aqueous solution of  $Na_2CO_3$  was added at room temperature and stirred for 1 h. The solution was extracted with EA. The collected layer was dried over  $MgSO_4$ , then filtered and concentrated under reduced pressure. The crude product was purified by silica-gel column chromatography using EA/PE (1/40, v/v) as eluent. A yellow solid was obtained in 77% yield.  $^1H$  NMR (400 MHz,  $CDCl_3$ ):  $\delta$  7.17-7.10 (m, 11H), 7.06-6.99 (m, 8H);  $^{13}C$  NMR (101 MHz,  $CDCl_3$ ):  $\delta$  164.01, 145.40, 143.13, 143.08, 142.94, 142.78, 139.27, 132.38, 132.15, 131.35, 131.29, 128.09, 128.05, 127.86, 127.12, 126.99, 126.96, 125.88, 124.55; HRMS (MALDI-TOF)  $m/z$ :  $[M]^+$  calcd. for  $C_{27}H_{19}N$ , 357.1500; found, 357.1512; IR (KBr,  $\nu$ ,  $cm^{-1}$ ): 2118.3 ( $N\equiv C$ ).

**TPE-NC-Au:** Into a 100 mL flask were added of  $C_6F_5Au(tht)$  (506.0 mg), TPE-NC (400.0 mg) and DCM (30 mL). The flask was evacuated and flushed with dry nitrogen three times, then the mixture was stirred overnight at room temperature. After filtration and solvent evaporation, the crude product was purified by silica-gel column chromatography using DCM/PE (1/4, v/v) as eluent.  $^1H$  NMR (400 MHz,  $CDCl_3$ ):  $\delta$  7.28-7.27 (d, 2H), 7.21-7.10 (m, 11H), 7.04-6.99 (m, 6H);  $^{13}C$  NMR (101 MHz,  $CDCl_3$ ):  $\delta$  148.36, 144.16, 142.98, 142.75, 138.95, 133.25, 131.61, 131.59, 131.48, 128.49, 128.18, 127.71, 127.52, 127.52, 126.48;  $^{19}F$  NMR ( $CDCl_3$ ):  $\delta$  -114.8 (m, 2F, m-F), -158.1 (m, 1F, p-F), -162.2 (m, 2F, o-F); IR (KBr,  $\nu$ ,  $cm^{-1}$ ): 2208.8 ( $N\equiv C$ ).

## Acknowledgment

This work was financially supported by the National Natural Science Foundation of China (No. 51473092) and the Shanghai Rising-Star Program (No. 15QA1402500). The authors greatly acknowledge the support and valuable suggestions in SC-XRD measurements from Ms Xiao-Li Bao and Ms Ling-Ling Li of the Instrumental Analysis Center of Shanghai Jiao Tong University.

## References

- [1] C.Y. Li, X. Tang, L.Q. Zhang, et al., Reversible luminescence switching of an organic solid: controllable on-off persistent room temperature phosphorescence and stimulated multiple fluorescence conversion, *Adv. Opt. Mater.* 3 (2015) 1184–1190.
- [2] J.J. Zhang, Q. Zou, H. Tian, Photochromic materials: more than meets the eye, *Adv. Mater.* 25 (2013) 378–399.
- [3] J. Mei, J. Wang, A.J. Qin, et al., Construction of soft porous crystal with silole derivative: strategy of framework design, multiple structural transformability and mechanofluorochromism, *J. Mater. Chem.* 22 (2012) 4290–4298.
- [4] C.D. Dou, D. Chen, J. Iqbal, et al., Multistimuli-responsive benzothiadiazole-cored phenylene vinylene derivative with nanoassembly properties, *Langmuir* 27 (2011) 6323–6329.
- [5] G.Q. Zhang, J.W. Lu, C.L. Fraser, Mechanochromic luminescence quenching: force-enhanced singlet-to-triplet intersystem crossing for iodide-substituted difluoroboron-dibenzoylmethane-dodecane in the solid state, *Inorg. Chem.* 49 (2010) 10747–10749.
- [6] J. Luo, L.Y. Li, Y.L. Song, et al., A piezochromic luminescent complex: mechanical force induced patterning with a high contrast ratio, *Chem. Eur. J.* 17 (2011) 10515–10519.
- [7] Z. Chi, X.Q. Zhang, B.J. Xu, et al., Recent advances in organic mechanofluorochromic materials, *Chem. Soc. Rev.* 41 (2012) 3878–3896.

- [8] Q.K. Qi, J.Y. Qian, X. Tan, et al., Remarkable turn-on and color-tuned piezochromic luminescence: mechanically switching intramolecular charge transfer in molecular crystals, *Adv. Funct. Mater.* 25 (2015) 4005–4010.
- [9] W.Z. Yuan, Y.Q. Tan, Y.Y. Gong, et al., Synergy between twisted conformation and effective intermolecular interactions: strategy for efficient mechanochromic luminogens with high contrast, *Adv. Mater.* 25 (2013) 2837–2843.
- [10] Y.J. Dong, B. Xu, J.B. Zhang, et al., Piezochromic luminescence based on the molecular aggregation of 9,10-Bis ((E)-2-(pyrid-2-yl) vinyl) anthracene, *Angew. Chem.* 124 (2012) 10940–10943.
- [11] Z.Y. Ma, Z.J. Wang, M.J. Teng, et al., Mechanically induced multicolor change of luminescent materials, *Chem. Phys. Chem.* 16 (2015) 1811–1828.
- [12] J.Q. Shi, W.J. Zhao, C.H. Li, et al., Switching emissions of two tetraphenylethene derivatives with solvent vapor, mechanical, and thermal stimuli, *Chin. Sci. Bull.* 58 (2013) 2723–2727.
- [13] Z.J. Wang, Z.Y. Ma, Y. Wang, et al., A novel mechanochromic and photochromic polymer film: when rhodamine joins polyurethane, *Adv. Mater.* 27 (2015) 6469–6474.
- [14] J. Wang, J. Mei, R.R. Hu, et al., Click synthesis, aggregation-induced emission, E/Z isomerization, self-organization, and multiple chromisms of pure stereoisomers of a tetraphenylethene-cored luminogen, *J. Am. Chem. Soc.* 134 (2012) 9956–9966.
- [15] K.W. Huang, H.Z. Wu, M. Shi, et al., Reply to comment on ‘aggregation-induced phosphorescent emission (AIE) of iridium (III) complexes’: origin of the enhanced phosphorescence, *Chem. Commun.* (2009) 1243–1245.
- [16] M. Ouyang, L.L. Zhan, X.J. Lv, et al., Clear piezochromic behaviors of AIE-active organic powders under hydrostatic pressure, *RSC Adv.* 6 (2016) 1188–1193.
- [17] J. Yang, Z.C. Ren, Z.L. Xie, et al., AIEgen with fluorescence-phosphorescence dual mechanoluminescence at room temperature, *Angew. Chem.* (2017) DOI: 10.1002/ange.201610453.
- [18] L. Wang, K.Q. Ye, H.Y. Zhang, Organic materials with hydrostatic pressure induced mechanochromic properties, *Chin. Chem. Lett.* 27 (2016) 1367–1375.
- [19] J.Q. Han, J.Y. Sun, Y.P. Li, et al., One-pot synthesis of a mechanochromic AIE luminogen: implication for rewritable optical data storage, *J. Mater. Chem. C* 4 (2016) 9287–9293.
- [20] B.J. Xu, W.L. Li, J.J. He, et al., Achieving very bright mechanoluminescence from purely organic luminophores with aggregation-induced emission by crystal design, *Chem. Sci.* 7 (2016) 5307–5312.
- [21] C.X. Shi, Z.Q. Guo, Y.L. Yan, et al., Self-assembly solid-state enhanced red emission of quinolinemalononitrile: optical waveguides and stimuli response, *ACS Appl. Mat. Interfaces* 5 (2012) 192–198.
- [22] T.Q. Xie, B.C. Zhang, X.P. Zhang, et al., AIE-active  $\beta$ -diketones containing pyridiniums: fluorogenic binding to cellulose and water-vapour-recoverable mechanochromic luminescence, *Mater. Chem. Front.* (2017) DOI: 10.1039/c6qm00187d.
- [23] G.G. Shan, H.B. Li, J.S. Qin, et al., Piezochromic luminescent (PCL) behavior and aggregation-induced emission (AIE) property of a new cationic iridium (III) complex, *Dalton Trans.* 41 (2012) 9590–9593.
- [24] X.L. Luo, J.N. Li, C.H. Li, et al., Reversible switching of the emission of diphenyldibenzofulvenes by thermal and mechanical stimuli, *Adv. Mater.* 23 (2011) 3261–3265.
- [25] X.Q. Zhang, Z.G. Chi, Y. Zhang, et al., Recent advances in mechanochromic luminescent metal complexes, *J. Mater. Chem. C* 1 (2013) 3376–3390.
- [26] X. Zhang, J.Y. Wang, J. Ni, et al., Vapochromic and mechanochromic phosphorescence materials based on a platinum(II) complex with trifluoromethylacetylide, *Inorg. Chem.* 51 (2012) 5569–5579.
- [27] K.A. King, P.J. Spellane, R.J. Watts, Excited-state properties of a triply ortho-metalated iridium(III) complex, *J. Am. Chem. Soc.* 107 (1985) 1431–1432.
- [28] Y. Kawamura, K. Goushi, J. Brooks, et al., 100% phosphorescence quantum efficiency of Ir(III) complexes in organic semiconductor films, *Appl. Phys. Lett.* 86 (2005) 071104.
- [29] L. Rodríguez, M. Ferrer, R. Crehuet, et al., Correlation between photophysical parameters and gold-gold distances in gold(I) (4-pyridyl) ethynyl complexes, *Inorg. Chem.* 51 (2012) 7636–7641.
- [30] T. Seki, K. Sakurada, M. Muromoto, et al., Photoinduced single-crystal-to-single-crystal phase transition and photosalt effect of a gold(I) isocyanide complex with shortening of intermolecular aurophilic bonds, *Chem. Sci.* 6 (2015) 1491–1497.
- [31] H. Ito, T. Saito, N. Oshima, et al., Reversible mechanochromic luminescence of  $[(C_6F_5Au)_2(\mu-1,4\text{-diisocyanobenzene})]$ , *J. Am. Chem. Soc.* 130 (2008) 10044–10045.
- [32] J.H. Liang, Z. Chen, J. Yin, et al., Aggregation-induced emission (AIE) behavior and thermochromic luminescence properties of a new gold(I) complex, *Chem. Commun.* 2013, 49, 3567–3569.
- [33] T. Seki, T. Ozaki, T. Okura, et al., Interconvertible multiple photoluminescence color of a gold(I) isocyanide complex in the solid state: solvent-induced blue-shifted and mechano-responsive red-shifted photoluminescence, *Chem. Sci.* 6 (2015) 2187–2195.
- [34] Z.J. Zhao, J.W.Y. Lam, B.Z. Tang, Tetraphenylethene: a versatile AIE building block for the construction of efficient luminescent materials for organic light-emitting diodes, *J. Mater. Chem.* 22 (2012) 23723–23740.
- [35] F. Wang, X. Li, S. Wang, et al., New  $\pi$ -conjugated cyanostilbene derivatives: synthesis, characterization and aggregation-induced emission, *Chin. Chem. Lett.* 27 (2016) 1592–1596.
- [36] Y.Q. Dong, J.W.Y. Lam, A.J. Qin, et al., Aggregation-induced emissions of tetraphenylethene derivatives and their utilities as chemical vapor sensors and in organic light-emitting diodes, *Appl. Phys. Lett.* 91 (2007) 011111.
- [37] X.F. Duan, J. Zeng, J.W. Lü, et al., Insights into the general and efficient cross McMurry reactions between ketones, *Org. Chem.* 71 (2006) 9873–9876.
- [38] D. Leifert, C.G. Daniliuc, A. Studer, 6-Aroylated phenanthridines via base promoted homolytic aromatic substitution (BHAS), *Org. Lett.* 15 (2013) 6286–6289.
- [39] T. Seki, Y. Takamatsu, H. Ito, A screening approach for the discovery of mechanochromic gold(I) isocyanide complexes with crystal-to-crystal phase transitions, *J. Am. Chem. Soc.* 138 (2016) 6252–6260.
- [40] K. Kawaguchi, T. Seki, T. Karatsu, et al., Cholesterol-aided construction of distinct self-organized materials from a luminescent gold(I)-isocyanide complex exhibiting mechanochromic luminescence, *Chem. Commun.* 49 (2013) 11391–11393.
- [41] A. Szytuła, D. Fus, B. Penc, et al., Electronic structure of RTX (R= Pr, Nd; T= Cu, Ag, Au; X= Ge, Sn) compounds, *J. Alloys. Compd.* 317 (2001) 340–346.
- [42] R. Uson, A. Laguna, M. Laguna, et al., *Inorg. Synth.* 26 (2007) 85–91.